

## Quantitative rRNA-Targeted Solution-Based Hybridization Assay Using Peptide Nucleic Acid Molecular Beacons<sup>∇†</sup>

Xu Li,<sup>1</sup> Eberhard Morgenroth,<sup>2,3</sup> and Lutgarde Raskin<sup>1\*</sup>

Department of Civil and Environmental Engineering, University of Michigan, Ann Arbor, Michigan 48109,<sup>1</sup> and Department of Civil and Environmental Engineering<sup>2</sup> and Department of Animal Sciences,<sup>3</sup> University of Illinois at Urbana-Champaign, Urbana, Illinois 61801

Received 4 May 2008/Accepted 16 September 2008

**The potential of a solution-based hybridization assay using peptide nucleic acid (PNA) molecular beacon (MB) probes to quantify 16S rRNA of specific populations in RNA extracts of environmental samples was evaluated by designing PNA MB probes for the genera *Dechloromonas* and *Dechlorosoma*. In a kinetic study with 16S rRNA from pure cultures, the hybridization of PNA MB to target 16S rRNA exhibited a higher final hybridization signal and a lower apparent rate constant than the hybridizations to nontarget 16S rRNAs. A concentration of 10 mM NaCl in the hybridization buffer was found to be optimal for maximizing the difference between final hybridization signals from target and nontarget 16S rRNAs. Hybridization temperatures and formamide concentrations in hybridization buffers were optimized to minimize signals from hybridizations of PNA MB to nontarget 16S rRNAs. The detection limit of the PNA MB hybridization assay was determined to be 1.6 nM of 16S rRNA. To establish proof for the application of PNA MB hybridization assays in complex systems, target 16S rRNA from *Dechlorosoma suillum* was spiked at different levels to RNA isolated from an environmental (bioreactor) sample, and the PNA MB assay enabled effective quantification of the *D. suillum* RNA in this complex mixture. For another environmental sample, the quantitative results from the PNA MB hybridization assay were compared with those from clone libraries.**

Accurate quantification of specific populations in complex microbial communities is important in many areas of microbiology. Today, real-time PCR-based techniques are often used for this purpose (45). Other PCR-based techniques, such as denaturing gradient gel electrophoresis (30) and terminal restriction fragment length polymorphism (29), have also been used to study microbial population dynamics, but they are less suitable as quantitative techniques (52). Oligonucleotide probe-based microbial quantification methods that do not rely on PCR usually target the small subunit rRNA and include quantitative membrane hybridization, quantitative fluorescence in situ hybridization (FISH), and phylogenetic microarrays. While membrane hybridization has been used successfully to study microbial population dynamics in a variety of complex microbial systems (39, 58), this technique is time consuming and labor intensive. Quantitative FISH also has been used effectively to quantify microbial populations (34, 59). However, in some applications, traditional FISH methods do not provide satisfactory quantitative results because of poor cell permeability for oligonucleotide probes (10), low accessibility of target sites in rRNA (18), or poor sensitivity when the cellular rRNA content is low (20). Microarray techniques have the potential to quantify rRNA extracted from environmental samples (16, 23), but reproducibility and specificity issues have not been addressed satisfactorily (37, 43).

The peptide nucleic acid (PNA) oligomer probe was studied

for its hybridization properties for the first time about 15 years ago (15). PNA differs from DNA in that it contains an electro-neutral polypeptide backbone while DNA includes a negatively charged sugar-phosphate backbone (31). The neutral backbone results in hybridization characteristics unique to PNA probes. For example, compared with traditional DNA probes, PNA probes bind more strongly to target nucleic acids (15) and are less dependent on the salt concentration used when hybridized to target DNA oligonucleotides (24). Furthermore, their hybridization kinetics are less affected by the secondary structure of target nucleic acids (3). These characteristics have allowed successful applications of PNA probes in various fields of microbiology (7, 11, 32, 54).

Apart from PNA-conferred improvements in probe composition, novel probe chemistries have also been devised for both DNA- and PNA-based probes. These include molecular beacons (MBs) (50, 55), adjacent fluorescence resonance energy transfer probes (9, 49), light-up probes (38, 46), and quenched autoligation probes (40, 41). The first DNA MB probes were developed by Tyagi and Kramer (50). A DNA MB contains a probe sequence complementary to the target region of nucleic acids and a stem structure consisting of a few nucleotides complementary to each other, allowing the DNA MB to form a stem-loop structure. A fluorophore is attached to one end of the DNA MB, while a quencher is bound to the other end. When no target nucleic acid is present, DNA MBs remain in their stem-loop configuration and the proximity of the quencher to the fluorophore results in limited or no fluorescence. When DNA MB probes bind to target nucleic acids, the stem-loop structure opens, resulting in an increase in the distance between the fluorophore and the quencher, and fluorescence can be detected. Thus, DNA MB probes fluoresce only upon hybridization to target nucleic acids, allowing for a solu-

\* Corresponding author. Mailing address: University of Michigan, Department of Civil and Environmental Engineering, 107 EWRE Building, 1351 Beal Ave., Ann Arbor, MI 48109-2125. Phone: (734) 647-6920. Fax: (734) 763-2275. E-mail: raskin@umich.edu.

† Supplemental material for this article may be found at <http://aem.asm.org/>.

∇ Published ahead of print on 26 September 2008.

TABLE 1. Specificity, coverage, and sequences of PNA MBs Dmonas0121 and Dsoma0848<sup>a</sup>

PNA MB	No. of sequences with perfect match in RDP	No. of targets in RDP <sup>b</sup>	Specificity <sup>c</sup>	Coverage <sup>d</sup>	Sequence (N terminus to C terminus)
Dmonas0121	61	58	33/61	33/58	TAMRA-E-AAGGTACGTTCCGATACA-K-K-DABCYL
Dsoma0848	29	22	20/29	20/22	TAMRA-E-TAGCTGCGGTACTAAAA-K-K-DABCYL

<sup>a</sup> Information on specificity and coverage was obtained through the Ribosomal Database Project II (RDP) on 22 May 2006 (12).

<sup>b</sup> The number of targets is defined as the number of sequences in RDP that belong to either *Dechloromonas* or *Dechlorosoma*.

<sup>c</sup> Specificity, number of targets in RDP with perfect match to the PNA MB/number of sequences in RDP with perfect match to the PNA MB.

<sup>d</sup> Coverage, number of targets in RDP with perfect match to the PNA MB/number of targets in RDP.

tion-based hybridization format (50). Hybridizations with DNA MBs exhibit several other advantages, such as a low background signal (28), high specificity (5), and high sensitivity (51). Because of these characteristics, DNA MB probes have been shown to be advantageous in applications in real-time PCR (35, 51), visualization of mRNA in living cells (6), and detection of nucleic acids in array techniques (4, 57) but have been less successful in quantifying rRNA in solution-based hybridizations (55).

PNA MB probes were developed to make use of the advantages of both PNA probes and the structure of MBs (33, 42). Different from DNA MBs, which contain a stem-loop structure, PNA MBs consist of only a loop structure. The stemless loop structure of PNA MBs simplifies probe design. PNA MBs are hydrophobic and therefore tend to fold to minimize the surface area in aqueous solution (42). In addition, the electrostatic interaction between two oppositely charged amino acids at each end may help bring the fluorophore and quencher into close proximity. So far, most of the studies of PNA MBs have focused on the hybridization of PNA MBs to DNA oligonucleotides (24, 26) or PCR products (35), except for a few studies in which 16S rRNA was used as targets in PNA MB hybridization (13, 55, 56). Even though PNA MBs are considerably more expensive than DNA MBs and are available from only one authorized vendor (Panagene, Daejeon, Korea), the use of PNA MBs in solution-based rRNA-targeted hybridizations showed much promise in a previous study (55). However, more work to evaluate reaction kinetics and hybridization specificity is needed before this technique can be used as a quantitative tool for environmental samples.

The present study addresses how probe sequence and hybridization conditions affect the kinetics of hybridization of PNA MBs to 16S rRNA and how well PNA MBs can differentiate target and nontarget rRNA, which affirms the potential of PNA MB hybridization as a quantitative assay in environmental studies.

## MATERIALS AND METHODS

**PNA MBs.** PNA MBs were designed in this study to target 16S rRNA of bacterial species within the genera *Dechloromonas* (S-G-Dmonas-0121-a-A-18, hereafter referred to as PNA MB Dmonas0121) and *Dechlorosoma* (S-G-Dsoma-0848-a-A-17, hereafter referred to as PNA MB Dsoma0848). Note that the type strain of the genus *Dechlorosoma*, *Dechlorosoma suillum* DSM 13638T, is nearly identical to the type strain of the genus *Azospira*, *Azospira oryzae* 6a3T, indicating that *D. suillum* is a later subjective synonym of *A. oryzae* (47). The two PNA MBs both contain the fluorophore tetramethylrhodamine (TAMRA) and the quencher 4-(4-dimethylaminophenylazo)-benzoic acid (DABCYL). The specificity, coverage, and sequences of the two PNA MBs are provided in Table 1. Sequences of the target sites in the 16S RNAs of target and nontarget species used in this study are presented in Table 2. A third PNA MB was designed to target the bacterial domain (S-D-Bact-0338-a-A-18, hereafter referred to as Bact0338) (55). All three PNA MBs were synthesized by Applied Biosystems (Foster City, CA) at the time. Upon receipt, PNA MBs were suspended in distilled deionized water at a concentration of 50  $\mu$ M and stored in polypropylene vials at  $-80^{\circ}$ C in the dark. These stock solutions were heated to  $50^{\circ}$ C for 10 min to ensure homogeneous solutions prior to preparing 10-fold dilutions to serve as working stocks. Working stocks were stored at  $-20^{\circ}$ C in the dark.

**RNA extractions.** Bacterial cultures of *Dechloromonas agitata* and *D. suillum* were purchased from the Deutsche Sammlung von Mikroorganismen und Zellkulturen GmbH (DSMZ 13637 and DSMZ 13638, respectively), and *Methylophilus methylotrophus* and *Marinospirillum minutulum* were purchased from the American Type Culture Collection (ATCC 53528 and ATCC 19193, respectively). Each of the four cultures was grown for 42 h in 10 ml of its recommended growth medium, and then 200  $\mu$ l of each culture was transferred to 200 ml of the growth medium. To reach their mid-exponential growth phase, *D. agitata* and *D. suillum* were grown aerobically at  $30^{\circ}$ C in DSMZ medium no. 1 for 14 and 18 h, respectively, *M. methylotrophus* was grown aerobically at  $30^{\circ}$ C in ATCC medium no. 1545 for 78 h, and *M. minutulum* was grown aerobically at  $26^{\circ}$ C in ATCC marine broth 2216 for 56 h. The environmental sample used in the spike-in experiment was collected from a laboratory-scale anaerobic bioreactor (58). The environmental samples used to compare PNA MB hybridization results with clone library results were collected from a laboratory-scale biologically active carbon reactor (X. Li, G. Upadhyaya, W. Yuen, J. Brown, E. Morgenroth, and L. Raskin, unpublished data).

Total RNA was extracted from centrifuged cell pellets using a phenol-chloroform-isoamyl alcohol extraction procedure (44), and the RNA was resuspended in distilled deionized water and stored at  $-80^{\circ}$ C. The concentrations of nucleic acids in the RNA extracts were measured spectrophotometrically using a NanoDrop ND1000 (NanoDrop Technologies, Wilmington, DE) at a wavelength of 260 nm. Furthermore, the quality of the RNA extracts was evaluated using

TABLE 2. Target sites in 16S rRNA of target and nontarget species included in this study for PNA MBs Dmonas0121 and Dsoma0848

Species <sup>a</sup>	Target site <sup>b</sup>	
	Dmonas0121	Dsoma0848
<i>Dechloromonas agitata</i>	5'-UGUAUCGGAACGUACCUU-3'	
<i>Dechlorosoma suillum</i> <sup>c</sup>	5'-U <b>AC</b> AUCGGAACGUAC <b>CA</b> -3'	5'-UUUUAGUACCGCAGCUA-3'
<i>Methylophilus methylotrophus</i>	5'-U <b>A</b> AUCGGAACG <b>GC</b> CUU-3'	5'- <b>CA</b> UGAGU <b>A</b> ACCGCAGCUA-3'
<i>Marinospirillum minutulum</i>		5'-UUUUAGU <b>A</b> ACCGCAGCUA-3'

<sup>a</sup> The first three species belong to the *Betaproteobacteria*, and *M. minutulum* belongs to the *Gammaproteobacteria*.

<sup>b</sup> The bold underlined nucleotides are mismatches to the PNA MBs presented in Table 1.

<sup>c</sup> The name *Dechlorosoma suillum* is a subjective synonym of the name *Azospira oryzae* (47).

TABLE 3. Hybridization conditions for various experiments<sup>a</sup>

Expt	Amt of 16S rRNA, fmol (species)	Amt of PNA MB, fmol (probe)	Sample vol, $\mu$ l	Hybridization condition	Instrument
Nonspecific opening of PNA MB	No RNA added	3,750 (Dsoma0848)	220	30, 50, and 70% formamide in hybridization buffers, hybridized at temp from 25 to 90°C with 5°C steps	Microplate
Kinetic expt	500	10,000 (Dsoma0848)	220	25°C, no formamide	Microplate
Melting-curve expt (including pure culture and artificial mixture expts)	7.5 <sup>b,c</sup>	150 (Dsoma0848 or Dmonas0121)	1.5	Hybridizations took place at a starting temp, and then the hybridization temp increased in a stepwise manner <sup>d</sup>	NanoDrop
Formamide expt	400	5,000 (Dmonas0121)	250	0–90% of formamide in hybridization buffers, and hybridized at 25°C	Microplate
Detection limit expt	0, 4.5, 6, and 7.5	150 (Dsoma0848)	1.5	68°C <sup>e</sup> for 100 min	NanoDrop
Spike-in expt	100 + $n$ ; $n$ <sup>f</sup>	500 (Dsoma0848)	1.5	68°C <sup>e</sup> for 100 min	NanoDrop
Environmental sample expt <sup>g</sup>	250	500 (Dsoma0848)	1.5	68°C <sup>e</sup> for 100 min	NanoDrop

<sup>a</sup> In nearly all experiments for PNA MBs Dmonas0121 and Dsoma0848, hybridization buffers contained 25 mM Tris-HCl and 10 mM NaCl. In the kinetic experiments testing various salt concentrations, the final NaCl concentrations in hybridization buffers varied from 0 to 500 mM. In the experiments using formamide to control hybridization stringency, the hybridization buffers contained 0 to 90% formamide.

<sup>b</sup> Diethyl pyrocarbonate (Sigma-Aldrich, St. Louis, MO) was added at 0.1% (vol/vol) to minimize RNA degradation in all melting-curve experiments.

<sup>c</sup> In the experiments using pure cultures, each 1.5- $\mu$ l sample contained 7.5 fmol of target or nontarget 16S rRNA. In the experiment with artificial mixtures of 16S rRNA, each 1.5  $\mu$ l of the mixture contained 7.5 fmol of target 16S rRNA (*D. suillum*) and 7.5 fmol of nontarget 16S rRNA (*M. minutulum*).

<sup>d</sup> The melting-curve experiments with pure cultures started at 22°C for 200 min, and then the temperature was increased with 3°C steps until 91°C. The melting-curve experiment with an artificial mixture started at 60°C for 100 min, and then the temperature was increased with 2 and 3°C steps until 81°C. In both experiments, fluorescence signals were measured 2 min after each increase in temperature.

<sup>e</sup> The hybridization temperature 68°C (in 0% formamide hybridization buffer) was determined experimentally (see Fig. 4 and Fig. 5).

<sup>f</sup> In the first series of rRNA mixtures, 100-fmol aliquots of 16S rRNA from an environmental sample (58) were spiked with  $n$  fmol of target 16S rRNA from *D. suillum*, resulting in various 16S rRNA percentages equal to  $n/(100 + n)$  (i.e., 0, 1, 2.5, 5, 10, 20, and 30%). In the second series, only  $n$  fmol of target 16S rRNA from *D. suillum* was used, corresponding to the amounts of 16S rRNA target in the first series.

<sup>g</sup> The environmental sample experiment also involved the use of PNA MB Bact0338. Hybridization buffer composition and hybridization conditions for Bact0338 were reported in reference 55.

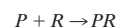
polyacrylamide gel electrophoresis (Jule Biotechnologies Inc., Milford, CT), and images of the gels were analyzed using Kodak (Rochester, NY) molecular imaging software (version 4.0.3K1). The concentration of 16S rRNA in each extract was calculated as the product of the total nucleic acid concentration estimated spectrophotometrically and the mass ratio of 16S rRNA to total nucleic acid obtained from the gel image analysis.

**Hybridizations.** The hybridization buffer composition and hybridization condition for PNA MB Bact0338 were adopted from the study by Xi et al. (55). The hybridization buffer used for PNA MBs Dmonas0121 and Dsoma0848 was modified from the same study and contained 25 mM Tris-HCl and 10 mM NaCl, except for specific experiments as described below. In the experiments testing various salt concentrations, hybridization buffers contained NaCl with final concentrations ranging from 0 to 500 mM. In the experiments using formamide for stringency control, hybridization buffers contained formamide ranging from 0 to 90% (vol/vol). In the experiments for which environmental samples were used, hybridization conditions were adopted from characterization experiments in this study or the study by Xi et al. (55). Detailed hybridization conditions for all experiments are summarized in Table 3.

Experiments to study the nonspecific opening of PNA MB (i.e., the response of PNA MB in the absence of rRNA), hybridization kinetics of PNA MB, and effects of formamide on hybridization stringency were performed in Costar standard 96-well microplates with black walls and clear bottoms (Corning 3651; Corning Incorporated, Corning, NY). Fluorescence signals in these experiments were measured using a Bio-Tek Synergy HT multidetection microplate reader (Winooski, VT) and expressed in relative fluorescence units (RFUs). Experiments to determine optimal hybridization temperatures (melting-curve experiments) and experiments with environmental samples were conducted in an Eppendorf ThermoStat Plus thermostat (Hamburg, Germany) for temperature control. Fluorescence signals in these experiments were measured using a NanoDrop ND3300 fluorospectrometer (NanoDrop Technologies, Wilmington, DE) and expressed in RFUs.

**Data analysis.** Net RFUs for hybridization of PNA to 16S rRNA were calculated as the differences between RFUs obtained with samples containing only PNA MB and RFUs from samples also containing 16S rRNA.

A pseudo-first-order model was used to fit the kinetic curves (36) for the formation of hybrids between PNA MB probes ( $P$ ) and target 16S rRNA ( $R$ ):



$$\frac{d[PR]}{dt} = -\frac{d[R]}{dt} = k_u[R] \quad (1)$$

where  $t$  is time,  $[R]$  is the concentration of target 16S rRNA in solution,  $[PR]$  is the concentration of hybrids, and  $k_u$  is the pseudo-first-order rate constant. This model assumes that the concentration of PNA MBs remains constant during hybridization. The assumption was satisfied by providing PNA MBs in 20-fold excess of 16S rRNA (Table 3). Integration of equation 1 yields

$$\frac{[R]_t}{[R]_0} = \exp(-k_u t) \quad (2)$$

where  $[R]_t$  and  $[R]_0$  are the 16S rRNA concentrations at time  $t$  and time zero, respectively. Next, the equation can be converted to

$$\frac{[R]_0 - [R]_t}{[R]_0} = 1 - \exp(-k_u t) \quad (3)$$

and further

$$\frac{[PR]_t}{[PR]_\infty} = 1 - \exp(-k_u t) \quad (4)$$

where  $[PR]_t$  and  $[PR]_\infty$  are the hybrid concentrations at time  $t$  and at time infinity, respectively. The value of  $[PR]_t$  was measured in RFU. The values of  $[PR]_\infty$  and  $k_u$  were simulated using the curve-fitting function in the software program KaleidaGraph (Synergy Software, Reading, PA). The two parameters,  $[PR]_\infty$  and  $k_u$ , provided information on the final hybridization signal and the apparent rate constant, respectively. The values of the apparent rate constants were subject to statistical analyses in Microsoft Excel using two-way analyses of variance with the sequence as one independent variable and the NaCl concentration as the other independent

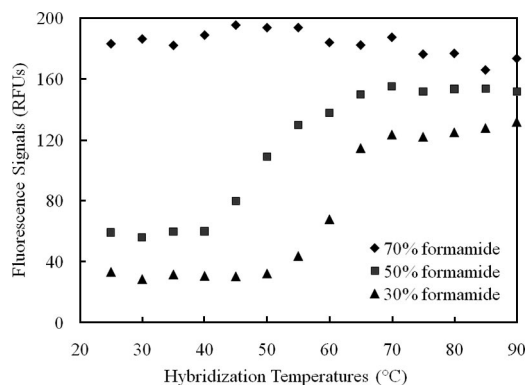


FIG. 1. Nonspecific opening of PNA MB Dsoma0848 due to the increases in the hybridization temperature and formamide concentration in hybridization buffers. No rRNA was present in this experiment.

variable. In this study, the units for the pseudo-first-order apparent rate constant are  $\text{RFU} \cdot \text{min}^{-1} \cdot \text{M}^{-1}$ . If RFU are converted to molarity, the units simplify to  $\text{min}^{-1}$ .

**Detection limit.** The detection limit of the PNA MB hybridization assay was determined using a standard procedure (17) with seven replicates for each 16S rRNA concentration included in the experiment (Table 3). In brief, measurement results from seven replicates were calculated for standard deviation ( $s$ ), a critical  $t$  value was obtained using a degree of freedom of 6 and a confidence level of 99% ( $t_{6, 0.99}$ ), and a method detection limit (MDL) was calculated as

$$\text{MDL} = t_{6, 0.99} \times s \quad (5)$$

## RESULTS

**Response of PNA MB in the absence of rRNA.** Before optimizing the stringency of hybridization between PNA MB and 16S rRNA by varying the hybridization temperature and the concentration of formamide in the hybridization buffer, the response of PNA MB to these two approaches in the absence of target or nontarget nucleic acid was evaluated. The PNA MBs exhibited substantial fluorescence without binding to target nucleic acids at high temperatures ( $>40^{\circ}\text{C}$  for 50% formamide and  $>50^{\circ}\text{C}$  for 30% formamide) and at all temperatures in 70% formamide (Fig. 1). This fluorescence signal is due to the opening of the loop structure of the PNA MB, a process referred hereafter to as nonspecific opening of PNA MB.

The effect of formamide on the nonspecific opening of PNA MB is more substantial than that of temperature (Fig. 1). For example, a formamide concentration of 70% resulted in higher fluorescence signals at low temperatures than a formamide concentration of 30% at high temperatures. In addition, an increase in temperature did not promote further nonspecific opening of PNA MB in the presence of 70% formamide. Because of the different patterns of fluorescence signals associated with the nonspecific opening of PNA MB, this nonspecific opening was monitored for all experiments in this study by including a control containing only PNA MB for each hybridization reaction. The fluorescence signals due to the nonspecific opening of PNA MB were subtracted from the fluorescence signals of samples containing 16S rRNA, and the resulting values are reported as net fluorescence signals using net RFUs.

**Hybridization kinetics. (i) Kinetics of hybridization to target and nontarget 16S rRNA.** Prior to the determination of optimal hybridization conditions, the kinetic properties of hy-

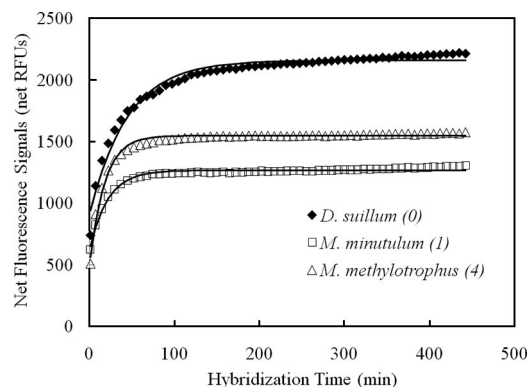


FIG. 2. A sample plot showing the kinetics of the hybridizations of PNA MB Dsoma0848 to target and nontarget 16S rRNA in the presence of 10 mM NaCl. The points are experimental data points, and the lines are curve fit based on a pseudo-first-order reaction model simulated in KaleidaGraph. The numbers in parentheses indicate the numbers of mismatches between 16S rRNA and PNA MB. The  $r^2$  values of the three curves in this figure ranged from 0.986 to 0.993.

bridizations of PNA MB were studied with various 16S rRNA sequences and in hybridization buffers of various NaCl concentrations. Five hundred fmol (1 fmol equals  $10^{-15}$  mol) of one target 16S rRNA (*D. suillum*) and two nontarget 16S rRNAs (*M. minutulum* and *M. methylotrophus*) were used in each hybridization reaction with 10,000 fmol of PNA MB Dsoma0848 (Table 3). This 20-fold excess of PNA MB to target and nontarget 16S rRNA resulted in hybridization reactions that exhibited pseudo-first-order kinetics, as indicated in Fig. 2 with good agreement between the simulation curves and the experimental data points. Hybridization of PNA MB Dsoma0848 to its target 16S rRNA (*D. suillum*) resulted in the highest final net fluorescence signals among the three hybridizations. Unexpectedly, the final signal of the hybridization to the 16S rRNA with four mismatches (*M. methylotrophus*) was higher than that from the hybridization to the 16S rRNA with one mismatch (*M. minutulum*). This phenomenon was also observed for some hybridization conditions in other kinetic experiments (Fig. 3a). In addition, the hybridization of PNA MB Dsoma0848 to nontarget 16S rRNAs exhibited faster kinetics and reached equilibrium faster than the hybridization to target 16S rRNA (Fig. 2).

**(ii) Effects of NaCl concentration on hybridization kinetics.** The effects of the monovalent cation concentration (i.e., sodium) on the kinetics of hybridization of PNA MB to 16S rRNA were studied by plotting final net fluorescence signals and apparent rate constants for various NaCl concentrations (Fig. 3). As the NaCl concentrations increased, final net fluorescence signals dropped substantially in hybridizations with both target and nontarget 16S rRNA (Fig. 3a). The maximum difference between the final net fluorescence signals for targets and nontargets was obtained at a NaCl concentration of 10 mM (Fig. 3a). Therefore, a NaCl concentration of 10 mM was chosen for subsequent experiments.

The apparent rate constants also decreased as the NaCl concentration increased (Fig. 3b). In addition, the apparent rate constants for the target were lower than those of the nontargets at all the NaCl concentrations tested, although this

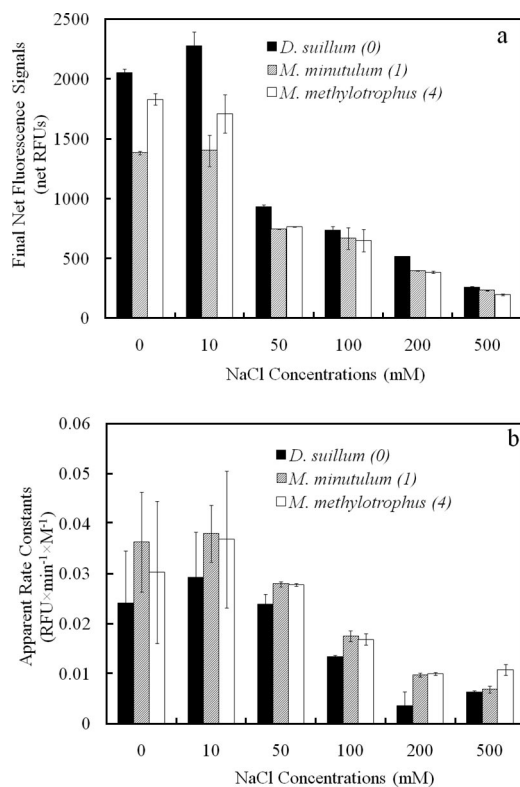


FIG. 3. The effects of NaCl concentrations in hybridization buffers on final net fluorescence signals (a) and apparent rate constants (b) from hybridizations of PNA MB Dsoma0848 to target and nontarget 16S rRNA. Mean values of duplicates are reported, and the error bars represent the range of the duplicates. The numbers in parentheses indicate the numbers of mismatches between 16S rRNA and PNA MB.

difference was not statistically significant. In the two-way analysis-of-variance tests, the NaCl concentration—an independent variable—appeared to have a significant effect on the apparent rate constants ( $P < 0.05$ ). In contrast, sequence—the other independent variable—did not have a significant effect on the apparent rate constant ( $P = 0.24$ ). The interaction between the two independent variables was not significant, either ( $P = 0.99$ ). The slower overall kinetics of the hybridization with target rRNA did not allow elimination of signal from nontargets using a kinetic approach.

**Optimization of hybridization conditions. (i) Stringency control using hybridization temperature.** Melting curves of the hybridizations of PNA MB Dsoma0848 with 16S rRNAs showed that at the lowest hybridization temperature of 22°C, target 16S rRNA (*D. suillum*) exhibited a higher net fluorescence signal than nontarget 16S rRNAs with one and four mismatches (*M. minutulum* and *M. methylotrophus*, respectively) (Fig. 4). Consistent with the order of final hybridization signals presented in the kinetic experiments (Fig. 2 and 3a), the net fluorescence signal from *M. methylotrophus* (four mismatches) was higher than that from *M. minutulum* (one mismatch) at 22°C and subsequent temperatures evaluated. As the temperature was increased, the net fluorescence signals of all three melting curves increased slightly and then decreased. Between 64 and 70°C, the three melting curves reached their minimum values. At about 68°C, the net fluorescence signal from *M. minutulum* was zero and the signal from *M.*

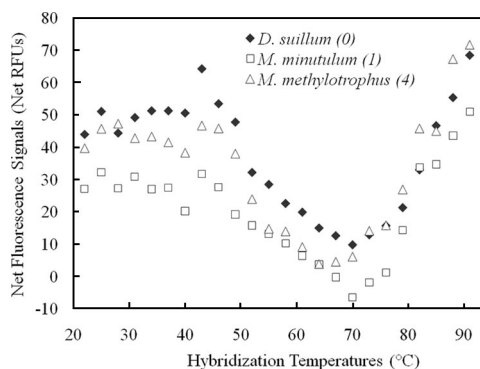


FIG. 4. Melting profiles of the hybridizations of PNA MB Dsoma0848 with its target and nontarget 16S rRNAs. The numbers in parentheses indicate the numbers of mismatches between 16S rRNA and PNA MB. The experiment was repeated, and similar profiles were obtained (data are shown in Fig. S1 in the supplemental material).

*methylotrophus* was low. Hence, 68°C was selected as the optimal hybridization temperature for PNA MB Dsoma0848.

After reaching minimum values, the net fluorescence signals increased for all three melting curves until the end of the experiment (Fig. 4). Such a phenomenon has not been reported in other studies with PNA MBs. Since the data in Fig. 4 were reported in net RFUs, it is likely that the presence of rRNA molecules—regardless of sequence—facilitated the nonspecific openings of PNA MBs at high temperatures.

To confirm the optimal hybridization temperature and demonstrate that elimination of signals from nontarget rRNA can be achieved in mixed cultures at optimized hybridization conditions, an artificial mixture containing equal amounts of 16S rRNA from target and nontarget with one mismatch (*D. suillum* and *M. minutulum*, respectively) was hybridized with PNA MB Dsoma0848 (Fig. 5). At the optimized hybridization temperature of 68°C, the net fluorescence signal from nontarget 16S rRNA with one mismatch was zero. The net fluorescence signals from the target and the artificial mixture were nearly identical, confirming that the nontarget 16S rRNA did not contribute to the signal. Thus, after optimization of hybridiza-

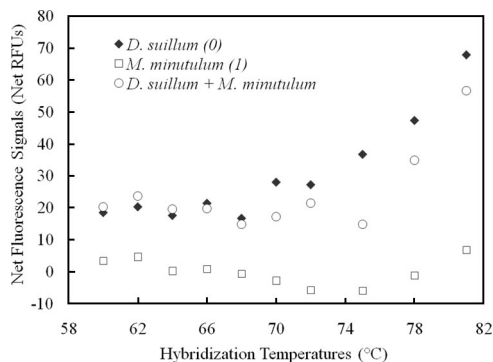


FIG. 5. Melting profiles of the hybridizations of PNA MB Dsoma0848 with 16S rRNAs of its target, nontarget, and an artificial mixture of the target and nontarget species. The numbers in parentheses indicate the numbers of mismatches between 16S rRNA and PNA MB. The experiment was repeated, and similar profiles were obtained (data are shown in Fig. S2 in the supplemental material).

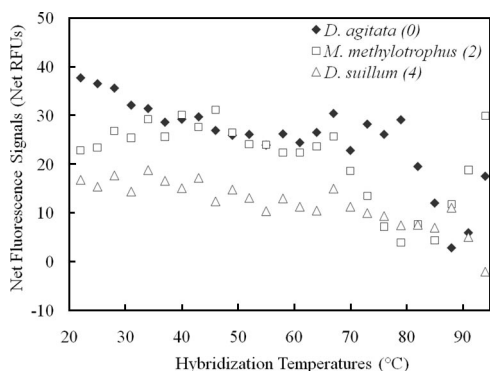


FIG. 6. Melting profiles of the hybridizations of PNA MB Dmonas0121 with its target and nontarget 16S rRNAs. The numbers in parentheses indicate the numbers of mismatches between 16S rRNA and PNA MB.

tion conditions, PNA MBs can be used to quantify target 16S rRNA in samples containing mixtures of rRNA, such as environmental samples. In addition, the fluorescence signal at 68°C in the melting-curve experiment started at 22°C (Fig. 4) was similar to the fluorescence signal at 68°C in the melting curve experiment started at 60°C (Fig. 5), which verified that the 2-min time period was sufficient for the hybridization to reach equilibrium after each increase in temperature (Table 3).

A similar melting-curve experiment was conducted for PNA MB Dmonas0121 with its target 16S rRNA (*D. agitata*) and nontarget 16S rRNAs with two and four mismatches (*M. methylotrophus* and *D. suillum*, respectively) (Fig. 6). Typical melting profiles were observed for target and nontarget 16S rRNAs. For the range of hybridization temperatures tested, the net fluorescence signals for nontargets were never completely eliminated (Fig. 6), even when formamide was added at 10 and 20% to the hybridization buffers (data not shown). Therefore, hybridization with PNA MB Dmonas0121 may result in substantial false-positive signals, especially for environmental samples containing low-abundance target populations. Hence, the addition of formamide to the hybridization buffer at a broad range of percentages was evaluated in order to minimize signals from nontarget rRNA.

(ii) **Stringency control using formamide.** The experiment performed to optimize the formamide concentration in the hybridization buffer for PNA MB Dmonas0121 resulted in typical sigmoid-shaped curves for both target 16S rRNA and nontarget 16S rRNA with two mismatches (*D. agitata* and *M. methylotrophus*, respectively) (Fig. 7). However, for formamide concentrations above approximately 40%, the net fluorescence signals were negative.

**Detection limit.** The detection limit of the hybridization assay using PNA MB Dsoma0848 was determined to be approximately 1.6 nM of 16S rRNA (*D. suillum*) under the optimized hybridization condition (i.e., a hybridization temperature of 68°C with no formamide in the hybridization buffer) (data not shown).

**Spike-in experiment.** The hybridization assay using PNA MB Dsoma0848 allowed quantification of target 16S rRNA (*D. suillum*) spiked at different concentrations to RNA extracted from an environmental sample. The hybridization response of

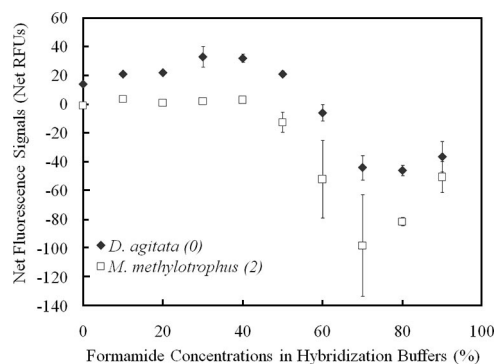


FIG. 7. Effect of formamide concentration at 25°C on the net fluorescence signals from the hybridizations of PNA MB Dmonas0121 with its target and nontarget 16S rRNAs. Mean values of duplicates are reported, and the error bars represent the range for the duplicates. The numbers in parentheses represent the numbers of mismatches between 16S rRNA and PNA MB.

PNA MB Dsoma0848 was linear over the range of 0 to 30% of relative abundance for the 16S rRNA spiked to the RNA extract from an environmental sample and for the corresponding target 16S rRNA alone (i.e., 0 to 43 fmol of target 16S rRNA; Fig. 8). However, the environmental RNA extract spiked with the different concentrations of target 16S rRNA resulted in higher hybridization responses.

**Environmental samples.** Two PNA MB hybridization assays using Dsoma0848 and Bact0338 were used to quantify the 16S rRNA from *Dechlorosoma* spp. and the total bacterial population in two biomass samples collected from a laboratory-scale biologically active carbon reactor, which was operated for nitrate and perchlorate removal from groundwater. After normalizing the results from Dsoma0848 with the results from Bact0338 (data on individual standard curves not shown), it was determined that *Dechlorosoma* spp. accounted for 10.5 and 36.4% of the bacterial community in the two biomass samples. In comparison, 16S rRNA gene clone libraries indicated that the relative abundances of *Dechlorosoma* spp. were 0.6 and 10.1% in these two biomass samples, respectively (Li et al., unpublished).

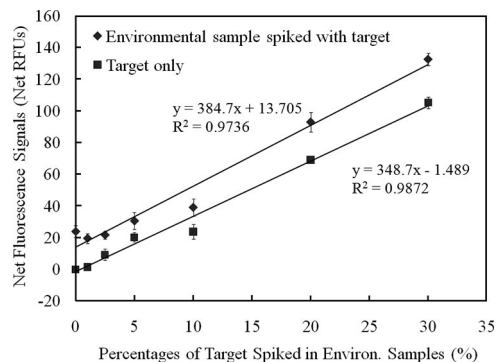


FIG. 8. Net fluorescence signals from the hybridizations of PNA MB Dsoma0848 with a series consisting of various amounts of target 16S rRNA (*D. suillum*) spiked to RNA extracted from an environmental sample and with a series of samples containing only target 16S rRNA corresponding to the amounts of 16S rRNA target in the first series. The error bars represent standard deviations for five replicates.

## DISCUSSION

In order to evaluate PNA MB hybridization as a tool to quantify specific 16S rRNA in environmental samples, hybridization kinetics and hybridization specificity were studied. Nonspecific opening of PNA MBs was observed under stringent hybridization conditions, making it necessary to include a control containing only PNA MB in each experiment. Despite the increase in the net fluorescence signal at high temperatures in melting curves, hybridizations at optimal temperatures can eliminate false-positive signals from nontarget rRNAs, differing in only one base from target rRNA (Fig. 4 and 5).

The kinetics of hybridization reactions depend on both forward and reverse reactions (i.e., association and dissociation processes). Solid surface hybridizations with linear DNA and PNA probes have been used to study association and dissociation rates. For example, using immobilized linear DNA oligonucleotide probes, Livshits and Mirzabekov demonstrated that the association rate constant was the same for target and nontarget DNA (27), and Dai et al. showed that nontargets exhibited higher dissociation rate constants than targets, which resulted in faster overall kinetics for nontarget (14). In contrast, immobilized linear PNA probes generally exhibited higher association rate constants and lower dissociation rate constants for targets than for nontargets (21). Unlike solid surface hybridizations, the solution-based hybridizations in this study do not allow separate analyses of association and dissociation processes. Based on conclusions presented by Jensen and coworkers (21), we suggest that the lower apparent rate constants in the hybridizations with target 16S rRNA (Fig. 2 and 3b) were the result of lower dissociation rate constants for target 16S rRNA.

The lower apparent rate constants for the hybridization of PNA MB with target 16S rRNAs demonstrated it was not feasible to use a kinetic approach to eliminate false-positive fluorescence signals due to nonspecific hybridization. Therefore, other approaches, such as optimizing the hybridization temperature and formamide concentration in the hybridization buffer, were used to control hybridization specificity for the PNA MBs Dmonas0121 and Dsoma0848. Before these approaches were tested, the salt concentration in the hybridization buffer was optimized.

Because 16S rRNAs were used as target molecules, the NaCl concentration in the hybridization buffer affected not only the hybridization between PNA MB Dsoma0848 and target molecules but also the secondary structures of the rRNA molecules. High salt concentrations (i.e., high ionic strength) in hybridization buffers favor the formation of RNA secondary structure and make the target sites in rRNA less accessible (48). A study of hybridizations between linear PNA probes and double-stranded-DNA oligonucleotide targets revealed that the initial association rates dropped as the NaCl concentrations increased from 20 to 50 mM (25). Unlike double-stranded-DNA oligonucleotides, 16S rRNAs exhibit a higher-order structure; thus, it was important to compare hybridization results for different NaCl concentrations.

It should be noted that the hybridization condition used in the kinetic experiments did not correspond to the optimized hybridization condition. As indicated above, the objectives of these experiments were to compare the kinetics of hybridiza-

tions of PNA MB to target and to nontarget 16S rRNAs, evaluate the effects of NaCl concentrations on PNA MB hybridization kinetics, and choose a NaCl concentration for experiments thereafter. Previous studies have evaluated the kinetics of hybridizations of PNA MB and DNA MB to target and nontarget DNA oligonucleotides (24) and target 16S rRNA (55). To our knowledge, this is the first study evaluating the effects of rRNA sequence and hybridization buffers on the kinetics of hybridizations of PNA MB to 16S rRNA.

The hybridization optimization experiments, with various hybridization temperatures and formamide concentrations in hybridization buffers, indicated the two PNA MB probes designed in this study required different optimization strategies (Fig. 4 to 7). A third PNA MB, Bact0338, previously designed and characterized by Xi and coworkers (55), was also included in our study. Xi et al. (55) defined the optimal formamide concentration as the condition that maximized the difference between the fluorescence signal of a hybridization reaction and the fluorescence signal of the control reaction containing only PNA MB. They demonstrated that hybridization under the optimized condition allowed differentiation of target and nontarget 16S rRNAs when their abundances were comparable. However, unpublished data from our study showed that the optimal hybridization condition as defined by Xi et al. (55) resulted in significant false-positive signals when the relative abundance of target 16S rRNA was low in an artificial mixture. Therefore, in the current study, melting-curve experiments were conducted for the PNA MB probe Bact0338 with target and nontarget 16S rRNAs to determine a condition that minimized the signal from nontargets. Unexpectedly, PNA MB Bact0338 exhibited melting profiles completely different from those shown in Fig. 4 and 6: the net fluorescence signals from both target and nontarget 16S rRNAs increased with hybridization temperatures (data not shown). Thus, we conclude that each newly designed PNA MB needs to be carefully characterized and may require different stringency control strategies.

The difference between the two series in Fig. 8 may be attributed to the presence of target 16S rRNA in the environmental sample. The environmental sample was collected from an anaerobic bioreactor, and the genus *Dechlorosoma* contains heterotrophic facultative anaerobic respiring bacteria (1). Alternatively, the difference may be the result of nonspecific hybridization and/or nonspecific opening of PNA MB due to binding to environmental substances in the samples. This possible nonspecific hybridization signal corresponded to about 5% of the total signal. In this experiment, we decided to spike RNA extracted from a pure culture of a target strain into RNA extracted from an environmental sample, rather than spiking target cells into an environmental sample followed by RNA extraction. The latter approach may overestimate the sensitivity of the method, because target cells grown in rich medium likely have higher levels of 16S rRNA than cells in environmental samples (22).

The relative abundance values of *Dechlorosoma* spp. determined using the 16S rRNA-targeted PNA MB hybridization assay and with the 16S rRNA gene-targeted clone library method were different. Both methods provided results that could be qualitatively linked to the performance of the bioreactor: the increase of *Dechlorosoma* spp. with time was consistent with improved perchlorate removal in the bioreactor (data

not shown). Although the results obtained with the two methods differed substantially, such differences are not unusual, especially when methods subject to PCR biases are involved (2). It should also be noted that the target biomarkers for the two methods were different: the solution-based hybridization assay targets 16S rRNA, whereas the clone library method targets 16S rRNA genes. Others have shown substantial differences when such quantitative results were compared (8, 19).

We observed that PNA MB in the absence of rRNA produced substantial fluorescence signals at high temperatures or high formamide concentrations (Fig. 1). Bonnet et al. proposed a three-conformation model for DNA MB probes (5). The authors demonstrated that there were three conformations of structured DNA MB: DNA MBs hybridized to RNA molecules, free DNA MBs that do not contribute to fluorescence signals, and randomly coiled free DNA MBs that fluoresce. According to Bonnet et al., the third conformation usually occurs at high temperatures when hybrids between probe and target nucleic acid have melted and the stem structure of DNA MB is broken. In the current study, although the structure of PNA MBs is different from that of DNA MBs, it is reasonable to speculate that the majority of PNA MBs are present in a randomly coiled free form at high temperatures. The observed increases in net fluorescence signals in the presence of target and nontarget rRNAs (Fig. 4 and 5) suggest that rRNA molecules, independently of sequence, facilitate the formation of the coil-free PNA MB.

The negative values in net fluorescence signals (Fig. 4 to 7) may result from a quenching effect of nucleic acids on fluorophores. A study by Wang et al. suggested a quenching effect on TAMRA, the same dye used in the PNA MBs Dmonas0121 and Dsoma0848, when the dye is in proximity of a guanosine near the target site (53). In the current study, the fluorescence signals were reported as net fluorescence signals, the difference between the signals from controls containing only PNA MB and the signals from corresponding samples also containing rRNA molecules. Because the quenching effect is absent in the controls, the subtraction caused negative signals in the net fluorescence signals. It was noticed that the negative net fluorescence signals were more evident in the formamide experiment (Fig. 7) than in the melting-curve experiments (Fig. 4 to 6). This might be related to the fact that formamide is more efficient in causing nonspecific opening of PNA MB than temperature in controls (Fig. 1). Future studies should focus on designing new PNA MBs that maintain their loop structure even at stringent conditions when target rRNA is not present.

#### ACKNOWLEDGMENTS

This work was supported by U.S. National Science Foundation grant no. BES-0123342.

We appreciate helpful discussions with Chuanwu Xi and critical reviews of the manuscript by Diane Holder and three anonymous reviewers. We also thank Peter Adriaens and Jeremy Semrau for access to equipment.

#### REFERENCES

- Achenbach, L. A., U. Michaelidou, R. A. Bruce, J. Fryman, and J. D. Coates. 2001. *Dechloromonas agitata* gen. nov., sp. nov. and *Dechlorosoma suillum* gen. nov., sp. nov., two novel environmentally dominant (per)chlorate-reducing bacteria and their phylogenetic position. *Int. J. Syst. Evol. Microbiol.* **51**:527–533.
- Acinas, S. G., R. Sarma-Rupavtarm, V. Klepac-Ceraj, and M. F. Polz. 2005. PCR-induced sequence artifacts and bias: insights from comparison of two 16S rRNA clone libraries constructed from the same sample. *Appl. Environ. Microbiol.* **71**:8966–8969.
- Armitage, B. A. 2003. The impact of nucleic acid secondary structure on PNA hybridization. *Drug Discov. Today* **8**:222–228.
- Bockisch, B., T. Grunwald, E. Spillner, and R. Bredehorst. 2005. Immobilized stem-loop structured probes as conformational switches for enzymatic detection of microbial 16S rRNA. *Nucleic Acids Res.* **33**:e101.
- Bonnet, G., S. Tyagi, A. Libchaber, and F. R. Kramer. 1999. Thermodynamic basis of the enhanced specificity of structured DNA probes. *Proc. Natl. Acad. Sci. USA* **96**:6171–6176.
- Bratu, D. P., B. J. Cha, M. M. Mhlanga, F. R. Kramer, and S. Tyagi. 2003. Visualizing the distribution and transport of mRNAs in living cells. *Proc. Natl. Acad. Sci. USA* **100**:13308–13313.
- Brehm-Stecher, B. F., J. J. Hyldig-Nielsen, and E. A. Johnson. 2005. Design and evaluation of 16S rRNA-targeted peptide nucleic acid probes for whole-cell detection of members of the genus *Listeria*. *Appl. Environ. Microbiol.* **71**:5451–5457.
- Brinkmeyer, R., K. Knittel, J. Jurgens, H. Weyland, R. Amann, and E. Helmke. 2003. Diversity and structure of bacterial communities in arctic versus antarctic pack ice. *Appl. Environ. Microbiol.* **69**:6610–6619.
- Cardullo, R. A., S. Agrawal, C. Flores, P. C. Zamecnik, and D. E. Wolf. 1988. Detection of nucleic-acid hybridization by nonradiative fluorescence resonance energy-transfer. *Proc. Natl. Acad. Sci. USA* **85**:8790–8794.
- Carr, E. L., K. Eales, J. Soddell, and R. J. Seviour. 2005. Improved permeabilization protocols for fluorescence in situ hybridization (FISH) of mycolic-acid-containing bacteria found in foams. *J. Microbiol. Methods* **61**:47–54.
- Chandler, D. P., and A. E. Jarrell. 2003. Enhanced nucleic acid capture and flow cytometry detection with peptide nucleic acid probes and tunable-surface microparticles. *Anal. Biochem.* **312**:182–190.
- Cole, J. R., B. Chai, R. J. Farris, Q. Wang, S. A. Kulam, D. M. McGarrell, G. M. Garrity, and J. M. Tiedje. 2005. The Ribosomal Database Project (RDP-II): sequences and tools for high-throughput rRNA analysis. *Nucleic Acids Res.* **33**:D294–D296.
- Coull, J. M., B. D. Gildea, and J. J. Hyldig-Nielsen. June 2001. Methods, kits and compositions pertaining to PNA molecular beacons. U.S. patent 6,528,267.
- Dai, H. Y., M. Meyer, S. Stepanians, M. Ziman, and R. Stoughton. 2002. Use of hybridization kinetics for differentiating specific from non-specific binding to oligonucleotide microarrays. *Nucleic Acids Res.* **30**:e86.
- Egholm, M., O. Buchardt, L. Christensen, C. Behrens, S. M. Freier, D. A. Driver, R. H. Berg, S. K. Kim, B. Norden, and P. E. Nielsen. 1993. Pna hybridizes to complementary oligonucleotides obeying the Watson-Crick hydrogen-bonding rules. *Nature* **365**:566–568.
- El-Fantroussi, S., H. Urakawa, A. E. Bernhardt, J. J. Kelly, P. A. Noble, H. Smidt, G. M. Yershov, and D. A. Stahl. 2003. Direct profiling of environmental microbial populations by thermal dissociation analysis of native rRNAs hybridized to oligonucleotide microarrays. *Appl. Environ. Microbiol.* **69**:2377–2382.
- Environmental Protection Agency. 1999, posting date. Protocol for EPA approval of new methods for organic and inorganic analytes in wastewater and drinking water. EPA 821-B-98-003. Environmental Protection Agency, Washington, DC.
- Fuchs, B. M., G. Wallner, W. Beisker, I. Schwipl, W. Ludwig, and R. Amann. 1998. Flow cytometric analysis of the in situ accessibility of *Escherichia coli* 16S rRNA for fluorescently labeled oligonucleotide probes. *Appl. Environ. Microbiol.* **64**:4973–4982.
- Gonzalez, J. M., R. Simo, R. Massana, J. S. Covert, E. O. Casamayor, C. Pedros-Alio, and M. A. Moran. 2000. Bacterial community structure associated with a dimethylsulfoniopropionate-producing North Atlantic algal bloom. *Appl. Environ. Microbiol.* **66**:4237–4246.
- Hahn, D., R. I. Amann, W. Ludwig, A. D. L. Akkermans, and K. H. Schleifer. 1992. Detection of microorganisms in soil after insitu hybridization with ribosomal-RNA-targeted, fluorescently labeled oligonucleotides. *J. Gen. Microbiol.* **138**:879–887.
- Jensen, K. K., H. Orum, P. E. Nielsen, and B. Norden. 1997. Kinetics for hybridization of peptide nucleic acids (PNA) with DNA and RNA studied with the BIAcore technique. *Biochemistry* **36**:5072–5077.
- Kerkhof, L., and B. B. Ward. 1993. Comparison of nucleic-acid hybridization and fluorometry for measurement of the relationship between RNA/DNA ratio and growth-rate in a marine bacterium. *Appl. Environ. Microbiol.* **59**:1303–1309.
- Koizumi, Y., J. J. Kelly, T. Nakagawa, H. Urakawa, S. El-Fantroussi, S. Al-Muzaini, M. Fukui, Y. Urushigawa, and D. A. Stahl. 2002. Parallel characterization of anaerobic toluene- and ethylbenzene-degrading microbial consortia by PCR-denaturing gradient gel electrophoresis, RNA-DNA membrane hybridization, and DNA microarray technology. *Appl. Environ. Microbiol.* **68**:3215–3225.
- Kuhn, H., V. V. Demidov, J. M. Coull, M. J. Fiandaca, B. D. Gildea, and M. D. Frank-Kamenetskii. 2002. Hybridization of DNA and PNA molecular beacons to single-stranded and double-stranded DNA targets. *J. Am. Chem. Soc.* **124**:1097–1103.

25. **Kuhn, H., V. V. Demidov, M. D. Frank-Kamenetskii, and P. E. Nielsen.** 1998. Kinetic sequence discrimination of cationic bis-PNAs upon targeting of double-stranded DNA. *Nucleic Acids Res.* **26**:582–587.
26. **Kuhn, H., V. V. Demidov, B. D. Gildea, M. J. Fiandaca, J. C. Coull, and M. D. Frank-Kamenetskii.** 2001. PNA beacons for duplex DNA. *Antisense Nucleic Acid Drug Dev.* **11**:265–270.
27. **Livshits, M. A., and A. D. Mirzabekov.** 1996. Theoretical analysis of the kinetics of DNA hybridization with gel-immobilized oligonucleotides. *Biophys. J.* **71**:2795–2801.
28. **Marras, S. A. E., S. Tyagi, and F. R. Kramer.** 2006. Real-time assays with molecular beacons and other fluorescent nucleic acid hybridization probes. *Clin. Chim. Acta* **363**:48–60.
29. **Marsh, T. L.** 1999. Terminal restriction fragment length polymorphism (T-RFLP): an emerging method for characterizing diversity among homologous populations of amplification products. *Curr. Opin. Microbiol.* **2**:323–327.
30. **Muyzer, G.** 1999. DGGE/TGGE a method for identifying genes from natural ecosystems. *Curr. Opin. Microbiol.* **2**:317–322.
31. **Nielsen, P. E., M. Egholm, and O. Buchardt.** 1994. Peptide nucleic acid (Pna)—a DNA mimic with a peptide backbone. *Bioconjug. Chem.* **5**:3–7.
32. **Oliveira, K., G. W. Procop, D. Wilson, J. Coull, and H. Stender.** 2002. Rapid identification of *Staphylococcus aureus* directly from blood cultures by fluorescence in situ hybridization with peptide nucleic acid probes. *J. Clin. Microbiol.* **40**:247–251.
33. **Ortiz, E., G. Estrada, and P. M. Lizardi.** 1998. PNA molecular beacons for rapid detection of PCR amplicons. *Mol. Cell. Probes* **12**:219–226.
34. **Pernthaler, J., A. Pernthaler, and R. Amann.** 2003. Automated enumeration of groups of marine picoplankton after fluorescence in situ hybridization. *Appl. Environ. Microbiol.* **69**:2631–2637.
35. **Petersen, K., U. Vogel, E. Rockenbauer, K. V. Nielsen, S. Kolvræ, L. Bolund, and B. Nexø.** 2004. Short PNA molecular beacons for real-time PCR allelic discrimination of single nucleotide polymorphisms. *Mol. Cell. Probes* **18**:117–122.
36. **Podell, S., W. Maske, E. Ibanez, and E. Jablonski.** 1991. Comparison of solution hybridization efficiencies using alkaline phosphatase-labelled and <sup>32</sup>P-labelled oligodeoxynucleotide probes. *Mol. Cell. Probes* **5**:117–124.
37. **Pozhitkov, A. E., R. D. Stedtfeld, S. A. Hashsham, and P. A. Noble.** 2007. Revision of the nonequilibrium thermal dissociation and stringent washing approaches for identification of mixed nucleic acid targets by microarrays. *Nucleic Acids Res.* **35**:e70.
38. **Privat, E., T. Melvin, U. Asseline, and P. Vigny.** 2001. Oligonucleotide-conjugated thiazole orange probes as “light-up” probes for messenger ribonucleic acid molecules in living cells. *Photochem. Photobiol.* **74**:532–541.
39. **Raskin, L., J. M. Stromley, B. E. Rittmann, and D. A. Stahl.** 1994. Group-specific 16S ribosomal-RNA hybridization probes to describe natural communities of methanogens. *Appl. Environ. Microbiol.* **60**:1232–1240.
40. **Sando, S., and E. T. Kool.** 2002. Imaging of RNA in bacteria with self-ligating quenched probes. *J. Am. Chem. Soc.* **124**:9686–9687.
41. **Sando, S., and E. T. Kool.** 2002. Quencher as leaving group: efficient detection of DNA-joining reactions. *J. Am. Chem. Soc.* **124**:2096–2097.
42. **Seitz, O.** 2000. Solid-phase synthesis of doubly labeled peptide nucleic acids as probes for the real-time detection of hybridization. *Angew. Chem.-Int. Ed. Engl.* **39**:3249–3252.
43. **Small, J., D. R. Call, F. J. Brockman, T. M. Straub, and D. P. Chandler.** 2001. Direct detection of 16S rRNA in soil extracts by using oligonucleotide microarrays. *Appl. Environ. Microbiol.* **67**:4708–4716.
44. **Stahl, D. A., B. Flesher, H. R. Mansfield, and L. Montgomery.** 1988. Use of phylogenetically based hybridization probes for studies of ruminal microbial ecology. *Appl. Environ. Microbiol.* **54**:1079–1084.
45. **Suzuki, M. T., L. T. Taylor, and E. F. DeLong.** 2000. Quantitative analysis of small-subunit rRNA genes in mixed microbial populations via 5'-nuclease assays. *Appl. Environ. Microbiol.* **66**:4605–4614.
46. **Svanvik, N., G. Westman, D. Y. Wang, and M. Kubista.** 2000. Light-up probes: thiazole orange-conjugated peptide nucleic acid for detection of target nucleic acid in homogeneous solution. *Anal. Biochem.* **281**:26–35.
47. **Tan, Z., and B. Reinhold-Hurek.** 2003. *Dechlorosoma suillum* Achenbach et al. 2001 is a later subjective synonym of *Azospira oryzae* Reinhold-Hurek and Hurek 2000. *Int. J. Syst. Evol. Microbiol.* **53**:1139–1142.
48. **Tinoco, I., and C. Bustamante.** 1999. How RNA folds. *J. Mol. Biol.* **293**:271–281.
49. **Tsuji, A., H. Koshimoto, Y. Sato, M. Hirano, Y. Sei-Iida, S. Kondo, and K. Ishibashi.** 2000. Direct observation of specific messenger RNA in a single living cell under a fluorescence microscope. *Biophys. J.* **78**:3260–3274.
50. **Tyagi, S., and F. R. Kramer.** 1996. Molecular beacons: probes that fluoresce upon hybridization. *Nat. Biotechnol.* **14**:303–308.
51. **Vet, J. A. M., A. R. Majithia, S. A. E. Marras, S. Tyagi, S. Dube, B. J. Poesz, and F. R. Kramer.** 1999. Multiplex detection of four pathogenic retroviruses using molecular beacons. *Proc. Natl. Acad. Sci. USA* **96**:6394–6399.
52. **von Wintzingerode, F., U. B. Gobel, and E. Stackebrandt.** 1997. Determination of microbial diversity in environmental samples: pitfalls of PCR-based rRNA analysis. *FEMS Microbiol. Rev.* **21**:213–229.
53. **Wang, L., A. K. Gaigalas, J. Blasic, and M. J. Holden.** 2004. Spectroscopic characterization of fluorescein- and tetramethylrhodamine-labeled oligonucleotides and their complexes with a DNA template. *Spectrochim. Acta Mol. Biomol. Spectrosc.* **60**:2741–2750.
54. **Worden, A. Z., S. W. Chisholm, and B. J. Binder.** 2000. In situ hybridization of *Prochlorococcus* and *Synechococcus* (marine cyanobacteria) spp. with rRNA-targeted peptide nucleic acid probes. *Appl. Environ. Microbiol.* **66**:284–289.
55. **Xi, C. W., M. Balberg, S. A. Boppert, and L. Raskin.** 2003. Use of DNA and peptide nucleic acid molecular beacons for detection and quantification of rRNA in solution and in whole cells. *Appl. Environ. Microbiol.* **69**:5673–5678.
56. **Xi, C. W., L. Raskin, and S. A. Boppert.** 2005. Evaluation of microfluidic biosensor development using microscopic analysis of molecular beacon hybridization kinetics. *Biomed. Microdevices* **7**:7–12.
57. **Yao, G., and W. H. Tan.** 2004. Molecular-beacon-based array for sensitive DNA analysis. *Anal. Biochem.* **331**:216–223.
58. **Zheng, D., L. T. Angenent, and L. Raskin.** 2006. Monitoring granule formation in anaerobic upflow bioreactors using oligonucleotide hybridization probes. *Biotechnol. Bioeng.* **94**:458–472.
59. **Zhou, Z., M. N. Pons, L. Raskin, and J. L. Zilles.** 2007. Automated image analysis for quantitative fluorescence in situ hybridization with environmental samples. *Appl. Environ. Microbiol.* **73**:2956–2962.